Draft version July 4, 2012
Preprint typeset using LaTeX style emulateapj v. 5/2/11

RADIATIVE AND MOMENTUM BASED MECHANICAL AGN FEEDBACK IN A 3-DIMENSIONAL GALAXY EVOLUTION CODE

Ena Choi[1], Jeremiah P. Ostriker[1,2], Thorsten Naab[3] and Peter H. Johansson[4,5]
[1]Department of Astrophysical Sciences, Princeton University, Princeton, NJ 08544, USA
[2]IoA, Cambridge, UK
[3] Max-Planck-Institut für Astrophysik, Karl-Schwarzschild-Strasse 1, 85741 Garching, Germany
[4] Department of Physics, University of Helsinki, Gustaf Hällströmin katu 2a, FI-00014 Helsinki, Finland and
[5] Finnish Centre for Astronomy with ESO, University of Turku, Väisäläntie 20, FI-21500 Piikkiö, Finland

Draft version July 4, 2012

ABSTRACT

We study the growth of black holes (BHs) in galaxies using three-dimensional smoothed particle hydrodynamic simulations with new implementations of the momentum mechanical feedback, and restriction of accreted elements to those that are gravitationally bound to the BH. We also include the feedback from the X-ray radiation emitted by the BH, which heats the surrounding gas in the host galaxies, and adds radial momentum to the fluid. We perform simulations of isolated galaxies and merging galaxies and test various feedback models with the new treatment of the Bondi radius criterion. We find that overall the BH growth is similar to what has been obtained by earlier workers using the Springel, Di Matteo, & Hernquist algorithms. However, the outflowing wind velocities and mechanical energy emitted by winds are considerably higher ($v_{\rm w} \sim 1000 - 3000$ km s^{-1}) compared to the standard thermal feedback model ($v_{\rm w} \sim 50 - 100$ km s^{-1}). While the thermal feedback model emits only 0.1% of BH released energy in winds, the momentum feedback model emits more than 30% of the total energy released by the BH in winds. In the momentum feedback model, the degree of fluctuation in both radiant and wind output is considerably larger than in the standard treatments. We check that the new model of the BH mass accretion agrees with analytic results for the standard Bondi problem.

Subject headings: accretion, accretion disks – black hole physics – galaxies: active– galaxies: nuclei – galaxies: starburst – quasars: general

1. INTRODUCTION

Accretion of matter onto a supermassive black hole (SMBH) is believed to emit enormous amounts of electromagnetic, luminous radiation and drive powerful jets, winds or outflows of quasar (Lynden-Bell 1969; Rees 1984). The energy outputs emitted by accreting SMBHs at the centers of bulges and elliptical galaxies (Kormendy & Richstone 1995; Richstone et al. 1998) are believed to play an important role during galaxy formation and evolution, as revealed by many empirical correlations between their masses $M_{\rm BH}$ and host galaxy properties, e.g., the dispersion σ of the host galaxy (Gebhardt et al. 2000; Tremaine et al. 2002; Gültekin et al. 2009; Graham et al. 2011), bulge stellar mass (Dressler 1989; Kormendy 1993; Magorrian et al. 1998; Marconi & Hunt 2003; Gültekin et al. 2009), and the bulge binding energy (Aller & Richstone 2007; Barway & Kembhavi 2007). These correlations have led to the development of models where the SMBHs are linked by feedback from the central SMBHs, i.e., feedback via the mass ejection by winds or jets, or the emitted radiation regulates the mass accretion rate and the final SMBH mass. The feedback can be in the forms of radiatively or mechanically driven winds (Fabian 1999; Proga et al. 2000, 2008), or of radiative effects such as Compton heating and photoionization (Sazonov et al. 2005; Ciotti & Ostriker 2007), or of radiation pressure (DeBuhr et al. 2010, 2011a). Thermal feedback, heating by an unspecified mechanism has also been employed by many authors, e.g., Springel et al. (2005b); Hopkins et al. (2005); Johansson et al. (2009a,b).

In this rapidly developing field of active galactic nucleus (AGN) feedback, it is natural for large scale numerical simulations to explore first the simplest schemes. Thus physical processes, which cannot all be included in the first three-dimensional hydrodynamic simulations, have been treated in a selective fashion. For example, in Springel et al. (2005b, here after "SdMH05"), among the first who reproduced the AGN feedback in a three-dimensional smoothed particle hydrodynamics (SPH) code, the feedback was assumed to be purely thermal. That is, some fraction of the bolometric luminosity of accreting BHs is deposited as thermal energy to the neighboring gas particles via a mechanism that is not specified. The authors found that this thermal feedback treatment regulates and then terminates the further growth of the BH and expels gas from the central region in the galaxy in a quasar-driven outburst. This pioneering work, however, did not specify how the injected energy reaches the thermally heated gas particles. The conveyance of the energy is likely to be via either radiation or a wind, and in both cases momentum must be added with the thermal energy. If the energy is transferred via a wind with velocity $v_{\rm w}$, then the mass transfer may be significant and, since the ratio of momentum to energy scales as $1/v_{\rm w}$, the momentum transfer is correspondingly larger.

In a first attempt to study the relative importance of the different processes, utilizing one- and two-dimensional computations, it was found that mo-

mentum injection is the dominant mode of feedback (Ostriker et al. 2010, here after "OCCNP10"), because the very short cooling time of dense gas makes thermal input relatively inefficient. At the high densities of the central region of the galaxies, the cooling time of gas is sufficiently short in high resolution simulations, so that it cannot retain the injected thermal energy and efficiently convert it to kinetic energy. However, if the input to the surrounding fluid is via winds, then the return of mass and momentum to that fluid can be the dominant drivers which can reduce the accreted SMBH mass by up to a factor of 100 (OCCNP10). Other recent work by DeBuhr et al. (2010, 2011a), emphasizing the momentum input from optically thick radiation fields ($\sim \tau L/c$ with $\tau \sim 10$) has also found the dramatic effects of momentum input.

Observationally, around 15%–20% of bright quasars (Hewitt & Foltz 2003; Dai et al. 2008; Gibson et al. 2009) show outflows, where blueshifted broad absorption lines (BAL) are attributed to subrelativistic ($\sim 10,000$ km s^{-1}) mass ejection. According to the fraction of quasars with BAL winds together with the assumption that all quasars have outflows, the BAL outflows are wide, covering at least 20% of the solid angle. The radiation-driven winds from the detailed hydro simulation by Proga & Kallman (2004) cover $\sim \pi$ str, supporting this observational estimate. These outflows inject mass, momentum, and energy into the surrounding gas and are believed to be more efficient feedback agents of the host galaxies than relativistic jets, which drill through the ambient gas and put most of the energy into the intergalactic medium.

However, the effects of outflows to the host galaxies and larger cosmological structures are just beginning to be studied, because their mass ejection rates, energetics and sizes were largely undetermined. Adopting the recent measurements of mass ejection rates, and kinetic luminosities of the outflows from the absorption-line observations (Arav et al. 2008; Moe et al. 2009; Dunn et al. 2010), many authors introduced the kinetic AGN feedback in adaptive mesh refinement (AMR) simulations (Omma et al. 2004; Kim et al. 2011; Dubois et al. 2009) and in SPH simulations (Nayakshin & Power 2010; DeBuhr et al. 2012).

It has been shown that the average spectrum of AGN has a strong secondary peak in the high-energy X-rays ($\sim$ 50–100 keV) which is the main contributor to the Compton and secondary metal line heating (Sazonov et al. 2004). Some recent studies using one- and two-dimensional simulations including Ciotti & Ostriker (2007); Novak et al. (2011) considered the effect of momentum input, heating and radiation pressure from the AGN radiation. The recent SPH work by Hambrick et al. (2011) found that X-ray feedback, the heating and radiation pressure associated with the X-ray radiation field emitted from the BH, is more effective at suppressing star formation and BH mass growth compared to the traditional thermal feedback approach. The X-ray heating was also found to be effective in AMR simulations (Kim et al. 2011), as it heats the surrounding interstellar medium (ISM), keeps it hot for an extended duration of time, and effectively self-regulates the growth of the BH.

In many previous numerical studies of galaxy formation and evolution that only can resolve hundreds of pc to kpc scales, the accretion of gas onto BHs at the centers of AGNs occurs on unresolved scales. The Bondi–Hoyle–Lyttleton formalism (Hoyle & Lyttleton 1939; Bondi & Hoyle 1944; Bondi 1952) is commonly adopted, to obtain the BH mass accretion rate from the resolved larger scale properties of the ambient gas. This assumption has been made in studies of isolated galaxy and merging galaxies (e.g., SdMH05, Younger et al. 2008; Johansson et al. 2009b) and as well in cosmological simulations (e.g., Sijacki et al. 2007; Di Matteo et al. 2008; Booth & Schaye 2009; Teyssier et al. 2011; Dubois et al. 2012).

However, in most of the cases treated to date, the SPH smoothing length or the numerical resolution of the respective code is larger than the Bondi radius, i.e., the inner flow is numerically unresolved. The limitation of numerical and spatial resolution may introduce the unusual and unwanted effect—the neighboring gas particles around a BH at any distance from the BH can be accreted even though they are not gravitationally bound to the BH. This physically awkward treatment of the BH mass accretion may result in the very large growth of the central BH if we used the standard accretion algorithm without feedback. We will introduce a new treatment of gas particle accretion, "Bondi radius criterion", which statistically limits the accretion of mass to the gas particles which are within the Bondi radius.

The purpose of the current paper is to introduce (1) a modeling of AGN mechanical feedback via winds as observed in BAL systems that includes mass and momentum feedback, as well as thermal input; (2) the detailed treatment of radiative effects, i.e., X-ray radiative feedback; and (3) a modified BH accretion rate prescription using the Bondi radius criterion in the parallel TreeSPH-code GADGET. In this paper, we restrict our exploration to the simulations of isolated disk galaxies and merging galaxies, in order to better understand the specific properties of the new treatments. We reserve the follow-up papers for detailed analysis of merger simulations and cosmological simulations, to be compared with the results of observational papers.

This paper is structured as follows. In Section 2, we describe the simulation code, and discuss the BH feedback and new BH accretion prescription. We present the results and comparisons between our new model and standard prescription in Section 3. We summarize and discuss our findings in Section 4.

2. THE MODELS

2.1. *Numerical Code*

We perform the simulations using the parallel TreeSPH-code GADGET (Springel 2005). The code employs the Lagrangian SPH (see Monaghan 1992) technique and solves the equations of motion for the collisionless dark matter and star particles and gas. We include the radiative cooling for a primordial mixture of hydrogen and helium (Katz et al. 1996) and a spatially uniform time-independent local UV background (Haardt & Madau 1996). The gas of the ISM is assumed to be a two-phase medium of hot and cold gas (Mckee & Ostriker 1977; Springel & Hernquist 2003)

and stars form from a cold component embedded in sufficiently dense gas, i.e., $\rho > \rho_{\rm th}$ with the short-lived stars supplying an energy of 10^{51} erg to the surrounding gas per supernovae (SNe). This SN feedback heats the hot phase of the ISM and evaporates cold clouds, establishing a self-regulation cycle for star formation. SN-driven galactic winds are not included in this study.

We include all the basic aspects of the model for black hole (BH) accretion and feedback adopted in SdMH05, Springel et al. (2005a); Johansson et al. (2009b), and implement the momentum and mass feedback.

2.2. *Black Hole Feedback Model*

In the widely adopted SdMH05 model, the numerically unresolved accretion onto the BH is related to the large scale resolved gas distribution using a Bondi-Hoyle-Lyttleton parameterization (Hoyle & Lyttleton 1939; Bondi & Hoyle 1944; Bondi 1952). In very high resolution treatments where the Bondi radius ($R_B \sim 2GM_{\rm BH}/(c_s^2 + v^2)^{1/2}$) is resolved such as Ciotti et al. (2010); Novak et al. (2011); Barai et al. (2011), there is no need to specify the accretion rate as the hydro code with an appropriate inner boundary condition will correctly calculate the accretion rates. The accretion rate onto the BH in unresolved flows is estimated as

$$\dot{M}_{\rm B} = \frac{4\pi\alpha G^2 M_{\rm BH}^2 \rho}{(c_{\rm s}^2 + v^2)^{3/2}}, \quad (1)$$

where ρ and $c_{\rm s}$ are the density and sound speed of the surrounding gas, respectively. v is the velocity of the BH relative to the surrounding gas. Here α is a dimensionless parameter setting the efficiency of the accretion and it is conventionally set to be $\alpha = 100$ in SPH simulations on the grounds that the low spatial resolution currently available would otherwise limit the accretion rate to lower than the true value. Adopting $\alpha = 100$ gives reasonable results for the low resolution simulations discussed in SdMH05, and Johansson et al. (2009b), but in general α is resolution dependent. We adopt different values of α for the different resolutions, and details will be presented later in Section 3.1. Note that Equation (1) describes the accretion onto a point mass surrounded by adiabatic ($\gamma = 5/3$) gas with properties ρ, c, and v (in Equation (1)) far away from the BH ($r \to \infty$). Usually it is also assumed that the maximum accretion is limited to the Eddington rate given by

$$\dot{M}_{\rm edd} \equiv \frac{4\pi G M_{\rm BH} m_{\rm p}}{\epsilon_{\rm r}\sigma_{\rm T} c}. \quad (2)$$

Here $m_{\rm p}$ is the proton mass, $\sigma_{\rm T}$ is the Thomson cross-section and $\epsilon_{\rm r}$ is the radiative efficiency assumed to be a fixed value of 0.1 adopted from the mean value for radiatively efficient Shakura & Sunyaev (1973) accretion onto a Schwarzschild BH. This value is also supported by the global mass–energy relation pointed out by Soltan (1982) and Yu & Tremaine (2002). The accretion rate is then $\dot{M}_{\rm inf} = \min(\dot{M}_{\rm B}, \dot{M}_{\rm edd})$. The BHs are represented by collisionless "sink" particles, which feel only gravitational forces. The properties, including density, temperature, and the bulk velocity of the local gas around the BH, which then define the accretion rate, are estimated in a similar fashion to normal SPH particles.

Technically, the actual accretion of gas particles onto the BH particle is implemented using a stochastic approach (SdMH05). For each gas particle j around a BH, the probability of being absorbed by the BH is calculated as

$$p_j = \frac{w_j \dot{M}_{\rm inf} \Delta t}{\rho}, \quad (3)$$

where w_j is the kernel weight of the gas particle relative to the BH, $\dot{M}_{\rm inf}$ is the BH accretion rate and, Δt is the time step. The gas density ρ is measured at the position of the BH as

$$\rho = \sum_{i=1}^{N} m_i w_i, \quad (4)$$

where m_i denotes the gas particle mass, and N is the number of neighboring particles to the BH. From Equations (3) and (4), we see that the probability of the jth particle being accreted in time interval Δt is close to $p_j = \dot{M}_{\rm inf}\Delta t/m_{\rm gas}$, but influenced by the smoothing kernel of gas particle near the BH. The gas particle is swallowed by the BH when the probability p_j is larger than the generated random number uniformly distributed in the interval [0,1].

2.2.1. *Thermal Feedback*

In previous GADGET based studies, the feedback energy from the BH $E_{\rm feed}$ has typically been assumed to be some fraction $\epsilon_{\rm f}$ of the radiated luminosity $L_{\rm r}$ and couples thermally and isotropically to the surrounding gas as,

$$\dot{E}_{\rm feed} = \epsilon_f L_{\rm r} = \epsilon_f \epsilon_{\rm r} \dot{M}_{\rm inf} c^2. \quad (5)$$

Many authors (e.g., SdMH05) adopt a fixed value of $\epsilon_f = 0.05$ so that $\epsilon_{\rm w} = \epsilon_f \epsilon_{\rm r} = 5 \times 10^{-3}$, i.e., 0.5 percent of the accreted rest mass energy in total is available as thermal energy feedback. Utilizing this value for thermal feedback and adopting $\alpha = 100$, the normalization of the $M_{\rm BH} - \sigma$ was recovered by Di Matteo et al. (2005) in disk mergers simulations having a spatial resolution of $\epsilon_{\rm gas} = 0.1h^{-1}$ kpc and a mass resolution of $M_{\rm gas} \sim 6 \times 10^5 M_\odot$.

The corresponding feedback energy is distributed as thermal energy to the surrounding ~ 64 gas particles weighted by the SPH kernel. Note that the results may depend on the details of the numerical implementation. If ~ 128 particles are used of a given mass rather than ~ 64, the sound speed $c_{\rm s}^2$ would have been lower with corresponding increase of the accretion rate $\dot{M}_{\rm B}$ in Equation (1). What matters is the mass of the material into which the thermal energy is dumped. Thus, if the mass per particle were halved and the particle number was doubled the results would not change. In this standard approach, neither mass nor momentum is added to the ambient fluid by the BH and all energy that is added is via thermal energy.

2.2.2. *Momentum Feedback*

Accreting BHs are observed to emit broad-line winds that convey mass, energy, and momentum into the surrounding gas (de Kool et al. 2001; Moe et al. 2009; Dunn et al. 2010) and our goal is to include these observed flows in our numerical treatment. To implement

mechanical momentum and mass feedback, we define the inflowing and outflowing mass rates to be ($\dot{M}_{\rm inf}$, $\dot{M}_{\rm outf}$), and we use the following simple equations based on the conservation of mass, energy, and momentum (cf. OC-CNP10):

$$\dot{M}_{\rm acc} = \dot{M}_{\rm inf} - \dot{M}_{\rm outf}, \tag{6}$$

where $\dot{M}_{\rm acc}$ is the mass rate actually accreted onto the BH. We define the kinetic energy rate of the outflow $\dot{E}_{\rm w}$ as,

$$\dot{E}_{\rm w} \equiv \epsilon_{\rm w}\dot{M}_{\rm acc}c^2, \tag{7a}$$

$$= \frac{1}{2}\dot{M}_{\rm outf}v_{\rm w}^2, \tag{7b}$$

$$\dot{p} = \dot{M}_{\rm outf}v_{\rm w}, \tag{8}$$

where we have oversimplified matters by allowing only one wind velocity, $v_{\rm w}$, when in fact Equation (7b) requires $\langle v_{\rm w}^2\rangle$ and Equation (8) requires $\langle v_{\rm w}\rangle$ and $\epsilon_{\rm w}$ denotes the feedback efficiency, i.e., the wind efficiency in the momentum feedback model. Now, defining

$$\psi \equiv 2\epsilon_{\rm w}c^2/v_{\rm w}^2 = \dot{M}_{\rm outf}/\dot{M}_{\rm acc}, \tag{9}$$

we have, as solutions to Equations (6) - (8),

$$\dot{M}_{\rm acc} = \dot{M}_{\rm inf}\frac{1}{1+\psi}, \tag{10a}$$

$$\dot{M}_{\rm outf} = \dot{M}_{\rm inf}\frac{\psi}{1+\psi}, \tag{10b}$$

$$\dot{E}_{\rm w} = \epsilon_{\rm w}c^2\dot{M}_{\rm inf}\frac{1}{1+\psi}, \tag{10c}$$

$$\dot{p} = \dot{M}_{\rm inf}v_{\rm w}\frac{\psi}{1+\psi}. \tag{10d}$$

As we see from Equations (10a) and (10b), there is an important dimensionless quantity $\psi \equiv \dot{M}_{\rm outf}/\dot{M}_{\rm acc}$. In typical treatments of AGN feedback, ψ is assumed to be 0 in equations (10) implicitly assuming $v_{\rm w} \to \infty$, and so $\dot{M}_{\rm outf}$ and $\dot{p}$ are neglected. Thus, the two terms $\dot{E}_{\rm w}$ and $\dot{M}_{\rm acc}$ may be overestimated, and $\dot{p}$, the momentum input to the surrounding fluid is neglected. For example, if we adopt for the efficiency of generating mechanical energy the value $\epsilon_{\rm w} = \epsilon_f\epsilon_{\rm r} = 5\times10^{-3}$, as adopted by Springel (2005) and other authors, and we take $v_{\rm w} = 10,000$ km s^{-1} ($v_{\rm w,10}$) (Crenshaw et al. 2003; Moe et al. 2009), then we have $\psi = 9\ v_{\rm w,10}^{-2}$ and all of the neglected effects may in fact be dominant; 90 %, ($\psi/(1+\psi)$) of the inflowing mass may be ejected in a disk broad absorption line (BAL) wind and the mass and momentum input deposited in the ambient gas may dominate over the energy input.

To implement the actual output of mass, momentum, and energy, we modify the stochastic approach applied for the gas particle accretion on the BH shown in Equation (3). We first calculate a probability of being attracted into the central zone by the BH for each gas particle nearby using Equation (3) and determine its fate by generating a random number x_j in the interval [0,1]. For $x_j < p_j$, the gas particle is taken to be part of the inflow onto the BH. We then draw an independent random number y_j uniformly distributed in the interval [0,1] and compare it with $1/(1+\psi)$, the probability of being actually absorbed by the BH. For $y_j < 1/(1+\psi)$, the gas particle is accreted onto the BH. For $y_j > 1/(1+\psi)$, the gas particle is ejected with its wind velocity $v_{\rm w}$ and momentum.

We fix the wind velocity $v_{\rm w}$ to 10,000 km s^{-1} ($v_{\rm w,10}$) (Crenshaw et al. 2003; Moe et al. 2009) corresponding to a typical broad line wind. Together with our choice of $\epsilon_{\rm w} = 5\times10^{-4}$ (note that our energy coupling parameter $\epsilon_{\rm w}$ is 10 times smaller than the value used in other GADGET-2-based simulations), we have $\psi = 0.9$. That is, essentially one of the two particles inflowing to the BH is actually accreted by it, the other is driven out as part of the broad absorption line wind.

We emit a particle radially from the BH in the specified direction. We set the direction of wind to be parallel or anti-parallel to the direction of angular momentum ($\vec{r}\times\vec{v}$) of each gas particle, making it to be essentially perpendicular to the disk. The outflow is stronger perpendicular to disk (Proga & Kallman 2004) as the feedback is relatively inefficient in the accreting disk of BH which supplies a continuous fuel to the BH via inflow. In addition, the massive and geometrically thick nature of the molecular torus (e.g., Krolik & Begelman 1988; Tacconi et al. 1994) may restrict the outflow to the direction essentially parallel to the disk angular momentum vector.

AGN outflows can collide with and shock ambient gas, generating a momentum-driven flow. To mimic this phenomenon, we let the emitted wind particle share its momentum with the neighboring gas particles. With this "momentum share" treatment, the two nearest neighboring gas particles are expelled together with the wind particle. They have the same velocity increment, $\Delta v_{\rm w} \sim 10,000/3$ km s^{-1}, conserving the momentum. Sharing momentum with other particles via inelastic collisions, however, decreases the total kinetic energy increment (Equation (7b)) while preserving momentum. We deposit the residual energy into these three particles in thermal form so that total energy is conserved. Note that the wind particles can reach very high temperatures. The analysis of the number of momentum sharing particles will be discussed in the later sections.

Momentum sharing has two technical advantages. In general, high velocity particles will drive shocks. Similarly to SN remnants, the solution will approach a Sedov solution. However, with coarse mass and time resolution and having momentum share starts the cascade of transforming the $\sim$ 100% kinetic energy flux of the wind outflow to the $\sim$ 25% kinetic energy flux of the Sedov solution with twice the number of particles, a lower initial fraction of kinetic energy; and it makes the approach to the Sedov solution faster. Thus it makes us less sensitive to the problem of not having enough particles to correctly represent a hydrodynamic outflow. It also has computational advantages with regard to the time stepping. The standard Courant time step calculation implemented in the public release of GADGET might not guarantee fine enough time stepping for strong explosion problems (Springel 2010), and requires additional time-step limiter implementation (Saitoh & Makino 2009; Durier & Vecchia 2012). In momentum sharing, reducing the velocity of the wind by a factor of three, while maintaining the same momentum flux, reduces the need for short and expensive time steps

by the same factor, and our experiments have shown that if we perform solutions with high enough time and mass resolutions there is almost no difference between the two models. However, there is a great saving computationally in doing a momentum sharing when we are at low resolution.

In this approach mass, energy, and momentum are transferred to the ambient gas during AGN feedback and in addition to the usual efficiency parameter $\epsilon_{\rm w}$, we must introduce a parameter ψ (Equation (9)), the ratio of the outflow mass flux to the accreted mass flux, which is fixed by $\epsilon_{\rm w}$ and the wind velocity $v_{\rm w}$.

2.2.3. *X-ray Feedback*

We also consider the radiative feedback from the electromagnetic energy component of X-ray radiation from the BH. We first calculate the total radiation emitted from the location of the BH particle as

$$L_r = \epsilon_r \dot{M}_{\rm BH} c^2, \tag{11}$$

where the radiative efficiency $\epsilon_r = 0.1$ is adopted in all simulations (Ciotti & Ostriker 2007; Ciotti et al. 2009; Nobel et al. 2009). This luminosity is converted to a luminosity flux at the position of each particle by $F_r = L_r/4\pi r^2$, where r denotes the distance of the particle from the BH particle. We convert the flux to the net volume heating rate $\dot{E}$ by using the Sazonov et al. (2005) formulae, which describe the net heating rate per unit volume of a cosmic plasma in photoionization equilibrium with a radiation field characterized by the average quasar spectral energy distribution, as in Ciotti et al. (2010); Novak et al. (2011). We take into account Compton heating and photoionization heating as summarized below. The volume heating rate $\dot{E}$ in cgs units is given as:

$$\dot{E} = n^2 (S_1 + S_2), \tag{12}$$

where n is the proton density (in number). The Compton heating term S_1 is

$$S_1 = 4.1 \times 10^{-35} (1.9 \times 10^7 - T)\, \xi, \tag{13}$$

where the ionization parameter ξ is defined as

$$\xi \equiv \frac{L_r}{n(r) r^2}. \tag{14}$$

The sum of photoionization heating is given as

$$S_2 = 10^{-23} \frac{a\,(\xi/\xi_0)^b}{1 + (\xi/\xi_0)^b}, \tag{15}$$

where

$$a = \frac{1.7 \times 10^4}{T^{0.7}}, \tag{16}$$

$$b = 1.1 - \frac{1.1}{e^{T/1.8\,10^5}} + \frac{4 \times 10^{15}}{T^4}, \tag{17}$$

and finally

$$\xi_0 = \frac{1}{1.5/\sqrt{T} + 1.5 \times 10^{12}/\sqrt{T^5}} + \frac{4 \times 10^{10}}{T^2} \left[1 + \frac{80}{e^{(T-10^4)/1.5\,10^3}}\right]. \tag{18}$$

A speed-of-light delay in propagation from the BH is not included, since the effects of the delay should be small because of the small simulation scale ($\lesssim$ 50 kpc). We neither include radiative transfer nor optical depth effects for the hard X-ray radiation considered here.

However, we do include the electromagnetic momentum—the radiation pressure from the X-ray flux from the BH as in DeBuhr et al. (2010, 2011a). We model the radiation pressure by applying a total momentum per unit time of

$$\dot{p} = \dot{E}/c, \tag{19}$$

away from the BH particle to each gas particle, where $\dot{E}$ is the energy absorbed by the particle given the Sazonov et al. (2005) prescriptions. Here we neglect the effect of dust since the ISM generally has a low optical depth to hard X-rays. Hambrick et al. (2011) and Kim et al. (2011) recently studied the effects of X-ray radiation on the properties of massive elliptical galaxies. They found that X-ray feedback is more effective at suppressing star formation and BH mass growth compared to the traditional thermal feedback model.

2.3. *Eddington Force*

In the previous studies, the maximum accretion has been limited to the Eddington rate (Equation (2)) as shown in Section 2.2. Instead of manually limiting the mass accretion, we actually compute the Eddington force (EF) acting on the surrounding gas particles, directed radially away from the SMBH. We first calculate the luminosity as in Equation (11), and the flux at the position of the each particle by $F_r = L_r/4\pi r^2$ where r denotes the distance of the particle from the BH particle. Then, the total momentum change per unit time by the EF acting on the gas particles radially away from the SMBH particle is given as

$$\dot{p} = \frac{F_r N_e \sigma_T}{c}, \tag{20}$$

where N_e denotes the number of electrons associated with each gas particle and σ_T is the Thomson cross-section for the electron. When the SMBH has vigorous mass accretion bursts, i.e., above the Eddington mass accretion limit, the strong radiation pressure by the SMBH pushes the gas particles away, resulting in a lower density near the SMBH particle, which leads to the lower mass accretion rate. Since the Thompson cross-section is independent of frequency ($h\nu \ll m_e c^2$), no radiative transfer treatment is required; we assume that absorbed UV radiation is re-radiated as IR radiation.

2.4. *New BH accretion model*

2.4.1. *Bondi Radius Criterion*

The key to understanding the accretion process lies in correctly modeling the behavior of the accreting gas once it falls within the gravitational influence of the BH, the Bondi radius, $r_{\rm Bondi}$, defined as

$$r_{\rm Bondi} \equiv \frac{2GM_{\rm BH}}{{v_i}^2}, \tag{21}$$

where ${v_i}^2 = c^2 + {v_{\rm rel}}^2$, c and $v_{\rm rel}$ denote the sound speed and the relative velocity to the SMBH of the gas respectively. The Bondi radius divides the flow into two distinct

regions. Far outside of $r_{\rm Bondi}$, gas is hardly aware of the existence of the BH, and the flow is subsonic. On the other hand, inside the Bondi radius, gas has negative total energy and essentially plunges at free-fall. The Bondi radius in the spherical case being the place where the Mach number of the flow is unity. We note that heating that occurs within the Bondi radius cannot, by definition, affect the accretion rate since information cannot propagate upstream in a supersonic flow.

Applying the Bondi–Hoyle–Lyttleton formalism (Equation (1)) to the BH mass accretion rate assumes that the accretion onto the SMBH is commensurate with the accretion rate through the Bondi radius. In cases where the SPH smoothing length is greater than the Bondi radius, i.e., the inner flow is numerically unresolved, unusual effects can occur. To see what would happen if we used the standard accretion algorithm without feedback, we have made some artificial tests without any feedback mechanisms. We obtain a very large growth of the SMBH with $M_{\rm BH} \sim 10^{10} M_{\odot}$. The neighboring gas particles around a BH at any distance from the BH are accreted, even for particles which are not gravitationally bound to the BH.

To avoid any unphysical accretion from outside of the Bondi radius, we limit the accretion of mass to the gas particles statistically within the Bondi radius. With this Bondi radius criterion, gas particles can only be accreted when $r_i < r_{\rm Bondi}$, where r_i is the distance of the gas particle from the BH particle. When the mass of the BH is small, we cannot resolve the Bondi radius, i.e., the smallest resolvable length scale of our simulations, the gravitational softening length, is of a few tens of pc, whereas the Bondi radius is just a few pc when the BH mass is around $10^5 - 10^6 M_{\odot}$ ($r_{\rm Bondi}/{\rm pc} = 3.4\, M_{\rm BH,6}/v^2_{i,50}$ where $M_{\rm BH,6} = 10^6 M_{\odot}$ and $v_{i,50}$=50 km s^{-1}). In this case, we set the Bondi radius to be the smallest resolved scale, i.e., the gravitational softening length of the gas particles.

Since the gas mass distribution is smoothed with a kernel size h_i, we apply what we term "a soft cut of Bondi radius criterion". We allow the full accretion rate, only when the distance of the gas particle from the SMBH particles r_i is smaller than $r_{\rm Bondi} + r_{\rm soft}$. The gravitational softening length $r_{\rm soft}$, which avoids numerical singularities in the integral representation of the potential, is the smallest resolvable length scale and serves as the minimum bound to the smoothing length h_i. The soft Bondi probability $p_{\rm SB}$ as a function of the particle distance from the BH, for two cases of $r_B \leq r_{\rm soft}$ and $r_B > r_{\rm soft}$, is shown in Figure 1. When the soft Bondi limit (SB) is included, we reduce the probability of being absorbed by the BH for each gas particle (given as Equation (3)) used in the original code by the soft Bondi probability $p_{\rm SB}$, i.e., the final probability will be given as $p_{\rm final} = p_j \times p_{\rm SB}$. This treatment essentially limits the mass accretion only to the gas particles statistically within the Bondi radius.

2.4.2. *Free-fall modification of accretion rate*

In the standard version of the code the actual accretion of the gas particles is determined by the probability, which is only a function of the SPH smoothing kernel. We have altered this to include a dependence on the time

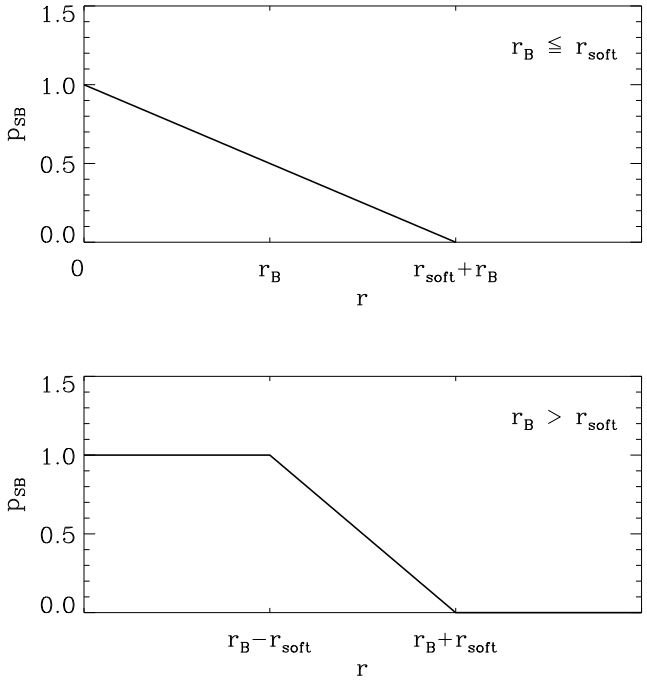

FIG. 1.— Soft Bondi probability of being absorbed by BH as a function of the particle distance r. The probability for the case when the Bondi radius $r_{\rm Bondi}$ is equal to the softening length $r_{\rm soft}$ shown in the upper panel, and one for the case when $r_{\rm Bondi}$ is larger than $r_{\rm soft}$ is shown below.

that it would take for the particle to be accreted allowing an extra factor of

$$p_{j,\rm ff} = \frac{\frac{1}{\tau_j}}{\frac{1}{N_{\rm sph}} \sum_{j=1}^{N_{\rm sph}} \frac{1}{\tau_j}}, \tag{22}$$

where $\tau_j = r_j/(c_{\rm s}^2 + v^2)^{1/2}$ is the free fall time and $N_{\rm sph}$ denotes the typical number of smoothing neighboring gas particles of the BH. We modify the probabilities (Equation (3)) to make them proportional to $p_{j,\rm ff}$, i.e., we make it more likely that nearby particles will be accreted in a given time step than more distant ones. When the free-fall (FF) modification is included, the final probabilities of the particles to be accreted by BH are given as $p_{\rm final} = p_j \times p_{j,\rm ff}$. where p_j denotes a probability of being absorbed by BH used in the original code (Equation (3)).

2.4.3. *Alternative averaging in the mass accretion calculation*

In the original implementation of Springel (2005), the BH mass accretion is calculated based on the physical quantities such as density, sound speed, and relative velocity of the surrounding gas of the BH as shown in Equation (1). These physical quantities for the BH particle are calculated from the ~ 64 neighboring gas particles using the SPH kernel. We can rewrite the Equation (1) as,

$$\dot{M}_{\rm B} = \frac{4\pi\alpha G^2 M_{\rm BH}^2 \langle\rho\rangle}{(\langle c_{\rm s}\rangle^2 + \langle v\rangle^2)^{3/2}}, \tag{23}$$

where angle brackets denote the averaging over the neighboring particles using SPH kernel. This method can be

unstable to the number of SPH neighboring particles chosen and it separately averages quantities in the numerator and the denominator of Equation (23). Suppose we made a run which used the 128 nearest particles instead of 64 nearest particles. It would have a different evolution, the soundspeed would be lower and so would the density. As noted earlier it is not the number of particles, per se that matters. If we halved the mass resolution and then moved to 32 particles we would keep the total mass into which the feedback energy was deposited a constant. We have performed this experiment and find that results are essentially unchanged. However, of course putting the energy into increasingly more mass would lower the feedback induced increase in $c_{\rm s}^2$ and change the Bondi rate after the use of Equation (1).

Our new averaging method for the calculation of the BH mass accretion "alternative averaging (AA)" does the calculation in both time and space on an individual particle basis and then averages the results over the nearest 64 particles in order to reduce the dependency on the number of SPH particles. With AA, we can rewrite Equation (1) as,

$$\dot{M}_{\rm B,AA} = \left\langle \frac{4\pi\alpha G^2 M_{\rm BH}^2 \rho}{(c_{\rm s}^2 + v^2)^{3/2}} \right\rangle, \tag{24}$$

where angle brackets denote the averaging over the SPH kernel. This method of performing the averaging is convergent because the added outer particles add progressively less and less.

2.4.4. *Fiducial BH mass accretion model*

In the fiducial model, we include all of the modifications we described for the BH mass accretion model, i.e., soft Bondi radius criterion (SB), free-fall modification (FF), and alternative averaging (AA). We first calculate the BH mass accretion rate using Equation (24) as shown above, and for the actual accretion of the gas particles onto the BH particle, we calculate a probability of being absorbed for each gas particle j as

$$p_{j,\rm final} = p_j \times p_{j,\rm SB} \times p_{j,\rm ff}. \tag{25}$$

We test our modified BH accretion model against the analytic Bondi solution in an idealized homogenous environment. As demonstrated in the Appendix we recover the Bondi solution.

3. RESULTS

3.1. *Galaxy Models*

The disk galaxies used in our study are set up in dynamical equilibrium and consist of a dark matter halo, a rotationally supported exponential disk of gas and stars, and a central bulge. The details of the model construction are summarized in SdMH05. We test and study the stability of the constructed galaxy feedback models with a representative sample of our disk galaxy models in isolation with $v_{\rm vir} = 160$ km s^{-1}, and $r_{\rm vir} = 160$ h^{-1} kpc corresponding to a virial mass of $M_{\rm vir} = 9.53 \times 10^{11}$ $h^{-1} M_\odot$. The dimensionless Hubble parameter is $h = 0.71$ such that the present-day Hubble parameter is $H_0 = 71$ km s^{-1} Mpc^{-1}. The Hernquist (1990) profile dark matter halos are constructed with the concentration parameter $c = 9$ of the corresponding Navarro–Frenk–White (NRW) halo (Navarro et al. 1997). The dark matter halo is then populated with exponential disks with a baryonic mass fraction of $m_d = 0.041$, so that a total disk mass $M_d = m_d M_{\rm vir}$ with a fractional gas content of $f_{\rm gas} = 0.2$ with the rest being stars.

To study the effects of numerical resolution, we use four models with different mass and spatial resolutions but with the same initial setup. The resolution details, including the number of particles, particle mass, and corresponding gravitational softening lengths are given in Table 1. The dimensionless accretion parameter in Equation (1) was set to $\alpha = 100$ in the previous studies (SdMH05; Johansson et al. 2009b), which correspond to our low-resolution model. This value is quite a bit higher than the theoretical value of $\alpha \sim 1$. This discrepancy is due to the numerical resolution limits, that is, the gas density and sound speed at the location of the SMBH are estimated over the large–scale, resulting in artificially low densities and high sound speed. The higher value of α has been adopted empirically to correct for this resolution effect. For the model with the higher numerical resolution, we adopt the smaller value of the dimensionless accretion parameter that can result in the similar scale of early accretion history of low resolution model with $\alpha = 100$. We run a series of simulations without any feedback prescription with the different values of α and adopt the α value that best reproduces the early accretion history of the low-resolution run with $\alpha = 100$. We turn off all the BH feedback to remove the resolution dependency of the feedback prescription. The adopted values of α for each resolution are shown in Table 1.

We summarize the properties of the models in Table 2. For reference, we first list the thermal feedback model "T", with the standard BH mass accretion and feedback model described in SdMH05. Note that model properties of standard model "T" in this paper are different from those of SdMH05, as we adopt "Very High" resolution as a standard resolution in this study, and the energy coupling efficiency $\epsilon_{\rm w} = 5 \times 10^{-4}$ which is 10 times smaller than the value adopted in SdMH05. We name our best proposed model with all the modifications that we have described "Fiducial". To isolate and compare the effects of each feedback model or modification, we include some simulations with one modification missing. We also include the "No Feedback" model: with no BH feedback in any form. Details of each model are shown in Table 2.

3.2. *Comparison of the different feedback mechanisms*

We first examine the effects of various feedback mechanisms on the evolution of the BHs and galaxies. Figure 2 shows the global star formation rate, the accretion rate onto the SMBH, and the evolution of the BH mass for the two different feedback models, the classical, thermal feedback (e.g., SdMH05), and our best proposed "Fiducial" model which has mechanical feedback with the X-ray heating and radiation pressure. Note that both models adopt the same feedback energy coupling efficiency $\epsilon_{\rm w} = 5 \times 10^{-4}$, which is 10 times smaller than the value adopted in SdMH05. A seed SMBH starts at rest in the center with mass of $M_{\rm BH} = 10^5 M_\odot$ in all models, and grows due to gas accretion during the simulation. Note that the growth of BH is essentially the same in the two models. Thus the primary results of SdMH05 and Di Matteo et al. (2005) with respect to the growth of

TABLE 1
Summary of the Numerical Resolution

Model	DM Particles	Disk Particles	$m_{\rm DM}$ ($h^{-1}M_\odot$)	$m_{\rm bar}$ ($h^{-1}M_\odot$)	$\epsilon_{\rm bar}$[a]	$\epsilon_{\rm DM}$[a]	α[b]
Low[c]	30,000	40,000	2.96×10^7	3.91×10^5	0.1	0.8	100
High	400,000	300,000	2.25×10^6	1.30×10^5	0.02	0.083	35
Very high	800,000	600,000	1.13×10^6	6.50×10^4	0.016	0.066	32.5
Ultra high	1,600,000	1,200,000	5.62×10^5	3.25×10^4	0.013	0.052	30

[a] Gravitational softening lengths in h^{-1} kpc.
[b] Dimensionless accretion parameter in Equation (1).
[c] Numerical resolution used in Springel et al. (2005b) corresponds to our low-resolution model.

TABLE 2
Summary of Model Properties

		Feedback								log	log	log	log	
	Model	T/M	X-Ray	X-Ray RP	FF	AA	SB	EF	NEL	$\Delta M_{\rm BH}$	$\Delta M_{\rm wind}$	$l_{\rm BH}^{\rm eff}$[a]	$L_{\rm wind}$[b]	$v_{\rm wind}$[c]
(1)	(2)	(3)	(4)	(5)	(6)	(7)	(8)	(9)	(10)	(11)	(12)	(13)	(14)	(15)
1	Thermal[d]	Thermal								7.47	8.92	–2.80	36.99	53.17
2	Fiducial[e]	Momentum	√	√	√	√	√	√	√	7.38	8.24	–2.66	40.72	1828.1
3	Fiducial w/o XRP	Momentum			√	√	√	√	√	7.96	9.22	–2.22	41.37	1287.9
4	Fiducial w/o EF	Momentum	√	√	√	√	√		√	7.41	8.56	–2.51	41.07	1727.2
5	Fiducial w/o SB	Momentum	√	√	√	√		√	√	7.54	8.71	–2.37	41.08	1743.9
6	N	No feedback								9.81	-	–3.86	-	-
7	N-SB	No feedback					√			8.89	-	–2.38	-	-

Notes. Model names indicate the activated physics (symbol √) in the simulations as detailed in Column 3–10. For example, in Model "Thermal" only thermal energy feedback is allowed, while in Model "N-SB", no feedback is included, with the soft Bondi (SB) treatment.

[a] $l_{\rm BH}^{\rm eff} \equiv L_{\rm BH,opt}^{\rm eff}/L_{\rm Edd}$ where $L_{\rm BH,opt}^{\rm eff}$ is the BH luminosity in the optical band after absorption, i.e., as it will be seen from infinity. The mean Eddington rates for last 1 Gyr are listed.
[b] The mechanical luminosity of the wind based on the wind mass rate and wind velocity measured at 5 kpc from BH for last ~ 1 Gyr. $L_{\rm wind} \equiv \dot{M}_{\rm wind} v_{\rm wind}^2/2$.
[c] Gas wind velocity at 5 kpc from BH in km s^{-1}.
[d] This model corresponds to the purely thermal feedback model discussed in SdMH05 (Springel et al. 2005b).
[e] Our best proposed "Fiducial" model.

central BHs during galaxy mergers are not substantially altered by the changes that we have introduced. Also, overall star formation rates of the two models are similar. However, the new model with mechanical feedback has more episodic star formation as in the mass accretion rate. Accretion rates and radiation output are much more variable in the new treatment with episodes of high accretion now reaching $L_{\rm BH}/L_{\rm Edd} \geq 0.1$. The mechanical feedback model spends a large fraction of time at relatively low Eddington accretion rate, coinciding with the observed broad-line active galaxies in the local universe (Greene & Ho 2007; Ho 2009; Kauffmann & Heckman 2009).

Moreover, the two models have quite different wind properties. In the mechanical feedback model, wind particles are ejected with the instantaneous disk wind velocity of $v_{\rm w} \sim 3000$ km s^{-1} (OCCNP10), while the heating from AGN feedback energy drives slow and hot outflows from galaxies in the thermal feedback model. The existence of a weak wind perpendicular to the plane of the disk in the vicinity of the BH was shown in SdMH05.

In order to compare the wind properties, we first measure the total outflow wind mass throughout the simulation by summing up the mass of the gas particles which pass through the plane $|z| = 5$ kpc, above and below the disk midplane. Then, we measure the velocity of the particle at each time step and calculate the corresponding mechanical luminosity as $L_{\rm wind} \equiv \dot{M}_{\rm wind} v_{\rm wind}^2/2$, i.e., the kinetic energy carried away by the outflowing winds. Temporal evolution of the wind properties (i.e., outflow rate, wind velocity and mechanical luminosity) of two representative models of thermal feedback (SdMH05) and the fiducial model is shown in Figure 3. Once the BHs reach similar masses, after about 3 Gyrs, the thermal feedback model develops a wind with about a factor of 10 higher outflow rate, but the velocity of the wind $v_{\rm w} \sim 100$ km s^{-1}, is a factor of 20 smaller compared to the mechanical feedback model. The high wind velocity ($v_{\rm w} \sim 2000$ km s^{-1}) in our fiducial model is consistent with the recent velocity measurement of mass outflows in local Seyferts (Fischer et al. 2011; Müller-Sánchez et al. 2011; Pounds & Vaughan 2011) which ranges from 700 km s^{-1} up to 3000 km s^{-1}.

The mechanical luminosities of the winds for two models are shown in the middle panel of Figure 3, and

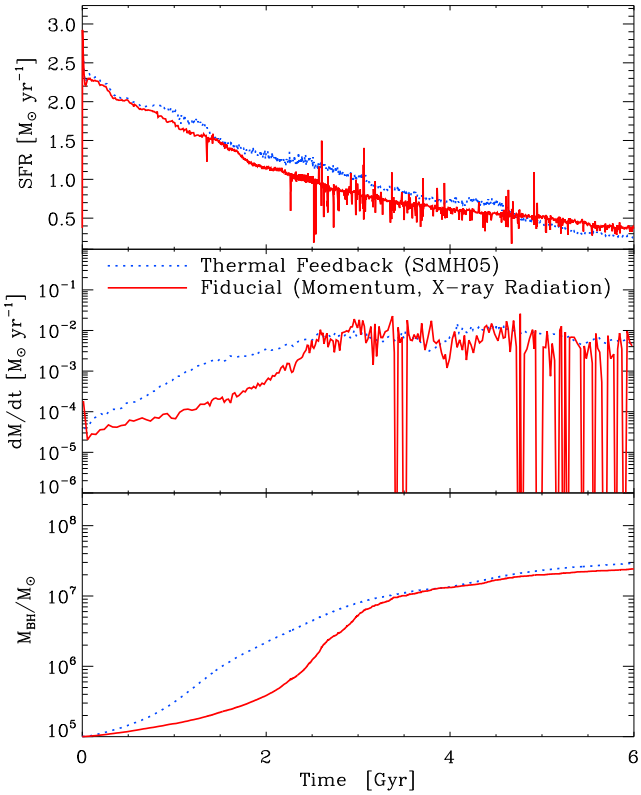

FIG. 2.— Comparison of the feedback models: classical thermal feedback (blue), and our best proposed "Fiducial" model which has momentum mechanical feedback with the X-ray heating and radiation pressure (red). Evolution of the global star formation rate (top), the accretion rate onto the black hole (middle) and the evolution of the black hole mass (bottom) for an isolated gas-rich disk galaxy. Note that both the star formation rate and the black hole growth are essentially similar in the new momentum driven treatment and the previous thermal feedback model. However, the degree of fluctuation in the mass accretion rate is greater in the momentum feedback model.

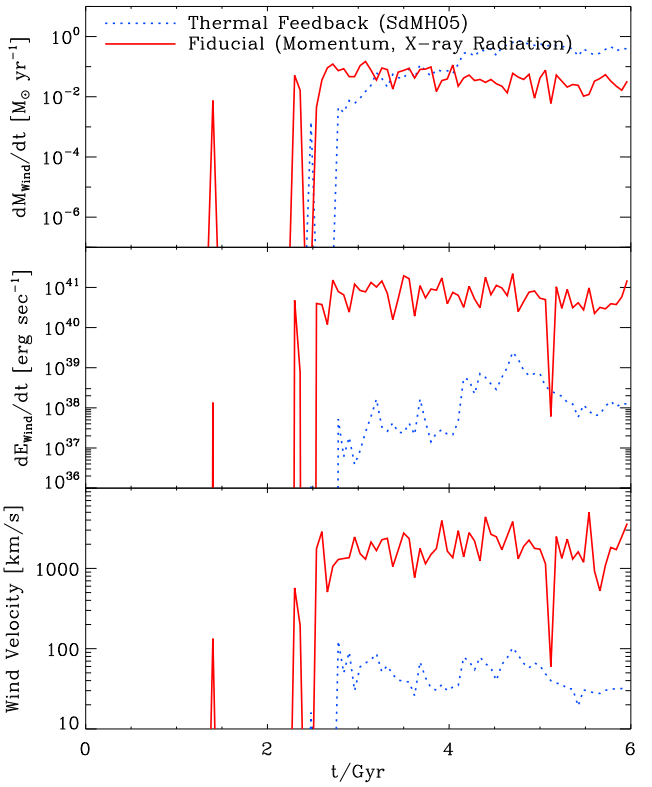

FIG. 3.— Top: the evolution of wind mass loss rate; middle: corresponding mechanical luminosities; bottom: gas wind velocities. All quantities are measured at 5 kpc from the SMBH, above and below the disk midplane. Note that the thermal feedback model has much smaller wind velocity, a factor of 20 smaller compared to the mechanical feedback model.

the averaged mechanical luminosities for last 1 Gyr are listed in Table 2. The thermal feedback model has considerably smaller mechanical luminosity $L_{\rm wind} \sim 10^{37}$ erg s^{-1}, because of its slow wind velocity. On the other hand, our fiducial model with mechanical feedback has strong outflow with $L_{\rm wind} \sim 10^{41}$ erg s^{-1}, which is consistent with the fact that large outflows with a kinetic power corresponding to a significant fraction of the AGN bolometric luminosity are commonly observed in X-ray observations of a number of quasars (mostly BAL systems) that reveal significant absorption (e.g., Chartas et al. 2003; Crenshaw et al. 2003; Pounds et al. 2003; Holt et al. 2008). The total kinetic energy carried away by the winds, i.e., the mechanical luminosities integrated over the entire simulation time for the thermal model is $\Delta E_{\rm wind} \sim 2.8 \times 10^{55}$ erg, while the momentum feedback model deposits $\Delta E_{\rm wind} \sim 8.3 \times 10^{57}$ erg into the ISM within 6 Gyr.

From a feedback energy coupling efficiency $\epsilon_{\rm w}$ which is an input parameter, and a total mass change for the BH, we calculate the energy released by the BH for the two cases using $\Delta E_{\rm mech} = \epsilon_{\rm w} \Delta M_{\rm BH} c^2$ and compare the ratios of the energy released in winds to the energy released by the BH, $\Delta E_{\rm wind}/\Delta E_{\rm mech}$. While the thermal feedback model emits only 0.1 % of the BH mechanical energy release in winds ($\Delta E_{\rm wind}/\Delta E_{\rm mech} = 0.0011$), the value rises to 38 % for the momentum feedback model, $\Delta E_{\rm wind}/\Delta E_{\rm mech} = 0.38$. That is, the mechanical energy put into momentum drives winds more efficiently than the energy put into heat.

Now we investigate the behavior of the two models for disk galaxy simulations at higher numerical resolution. However, such a study is complicated because of numerical resolution issues. In the previous studies using one-dimensional simulations, it was found that including the mass and momentum component has the largest effect on the final mass of the SMBH, reducing the final SMBH mass by a factor of up to 100 (OCCNP10). Turning on or off the energy input has relatively small effect, altering the SMBH mass only by a factor of two. But, in this three-dimensional study we have found that the momentum feedback is not more efficient than thermal feedback in protecting the SMBH from growth. However, the three-dimensional classic treatment has resolution effects that are difficult to correct because (1) the feedback energy is deposited outside of the Bondi radius whereas it is distributed within the Bondi radius in the much higher resolution one- and two- dimensional studies, and (2) the accretion is determined with the estimated gas density and sound speed averaged over the smoothing kernel, which is perhaps not the optimal procedure.

The results of the resolution dependency and the comparison of the wind properties of two feedback models are shown in Figure 4. Note that we adopt the smaller value of dimensionless accretion parameter α for the higher resolution runs as listed in Table 1. As described above,

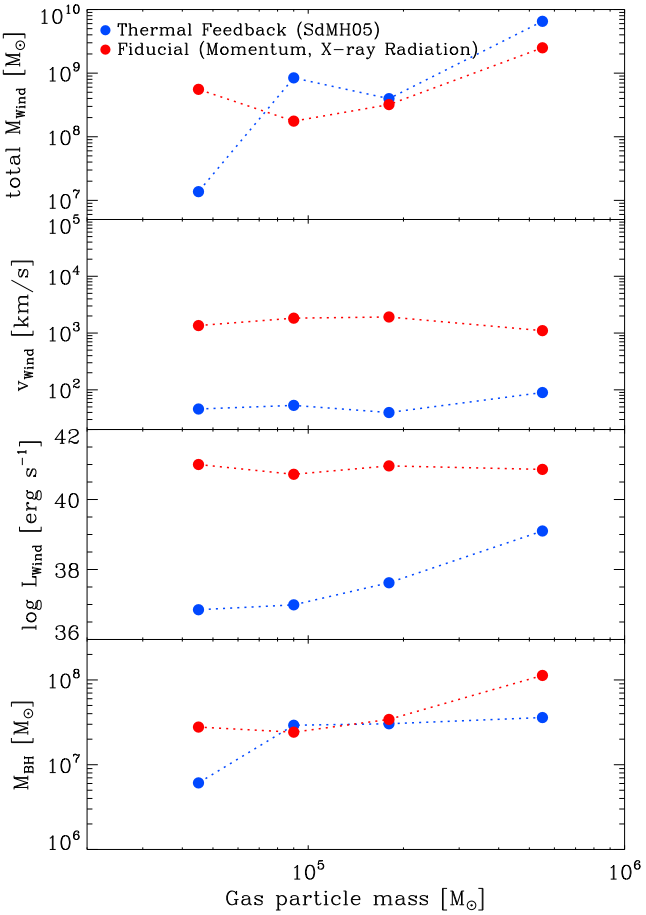

FIG. 4.— Outflow wind properties and the final SMBH mass for the thermal feedback (blue) and the momentum feedback (red) are shown as a function of resolution (gas particle mass). The total outflow wind mass throughout the simulations, the averaged outward wind velocity, the averaged mechanical luminosity for last 1 Gyr, and the final SMBH mass (from top to bottom) are shown. In the thermal feedback model, much weaken winds are generated in the highest resolution, since the injected feedback energy is quickly radiated away due to the very short cooling time of the gas.

we measure the outflow wind properties throughout the simulations at $|z| = 5$ kpc from BH, above and below the disk midplane. The measured wind masses, the time averaged wind velocities, and the averaged mechanical luminosities over the last 1 Gyr are shown for each feedback model as a function of the gas particle mass in Figure 4. The total amount of mass in the outflowing wind is resolution dependent in both models, but the effects of resolution appear to be larger in the thermal feedback model. While the momentum feedback model in the highest resolution simulation has less wind mass (by a factor of 10) compared to the lowest resolution one, the wind mass difference between thermal feedback models at different resolutions reaches 10^3. The wind velocity is resolution-independent for both feedback models, however thermal feedback models have much slower winds ($\sim 50 - 100$ km s^{-1}) compared to momentum feedback in all resolutions. The AGN-driven wind in the thermal feedback is also much slower than the velocity of the observed broad absorption line winds $\sim 10,000$ km s^{-1} (Crenshaw et al. 2003; Moe et al. 2009). In the case of the thermal feedback model at higher resolution, the shorter cooling time of dense gas makes thermal input increasingly inefficient at higher and higher numerical resolution.

In the case of the final mass of the BH (bottom panel of Figure 4), the effect of the resolution in the momentum feedback model is moderate, whereas the thermal feedback model has a factor of 10 smaller final mass in the highest resolution compared to one in the lowest resolution. For pure thermal feedback, we deposit the thermal feedback energy into the neighboring gas particles of the BH. The number of the affected neighboring gas particles is set to be the same for the different resolutions, therefore, in the higher resolution studies, we add energy into a smaller mass of the gas. In the higher resolution cases, gas particles in the central region have higher sound speed and lower density resulting in the lower BH accretion rate. However, the thermal feedback depends on the mass into which the energy is deposited, not on the number of particles. If the feedback energy were spread over constant mass by increasing the number of particles into which the thermal energy were added in the higher resolution study, the results would be essentially the same.

We compare the evolution of hot gas and X-ray emission of the two feedback models. Following Navarro et al. (1995), we assume that X-rays are produced by the cooling of hot and diffuse gas, and estimate the X-ray luminosity for each SPH gas particle as,

$$L_{\mathrm{X},i} = 1.2 \times 10^{-24} \frac{\rho_i m_{\mathrm{gas},i}}{(\mu m_p)^2} \left(\frac{kT_i}{1\mathrm{keV}} \right)^{1/2} \quad \mathrm{erg\ s^{-1}}, \quad (26)$$

where ρ_i, $m_{\mathrm{gas},i}$ and T_i are the density, mass, and temperature of the i th gas particle in cgs units, respectively, m_p is the proton mass, and μ is the mean molecular weight. The X-ray emission computed via Equation (26) for each SPH particle is a lower limit as it assumes that the primary mechanism for X-ray emission is thermal bremsstrahlung. We do not include the X-ray emission via metal-line cooling although it is the more efficient cooling mechanism for metal-enriched gas with a temperature of $\sim 10^6$ K and would produce more X-ray emission. We also assume that the central region of the galaxy remains obscured because of the large column density of intervening gas and dust, and calculate the total X-ray luminosity as

$$L_{\mathrm{X,tot}} = \sum_{j=1}^{N_{\mathrm{hot\ gas}}} L_{\mathrm{X},i}, \quad (27)$$

where the sum is over all hot and diffuse gas particles. Following Cox et al. (2006), we define the 'hot and diffuse gas' with a temperature of $T \geq 10^6$ K, and a density $\rho \leq 3.16 \times 10^{-3} M_\odot \mathrm{pc}^{-3}$, which corresponds to the critical density for star formation.

In Figure 5, we show where the SPH particles lie in the density-temperature plane with the calculated X-ray luminosities for both feedback models. In the thermal feedback model, the energy input by the accreting BHs generates collimated, hot and slow winds perpendicular to the disk plane. These wind particles leave from the high density and hot temperature tip of the distribution of gas in the density-temperature plane, and cool down slowly as they move outward. Due to their low velocity and high density, the cooling time is relatively

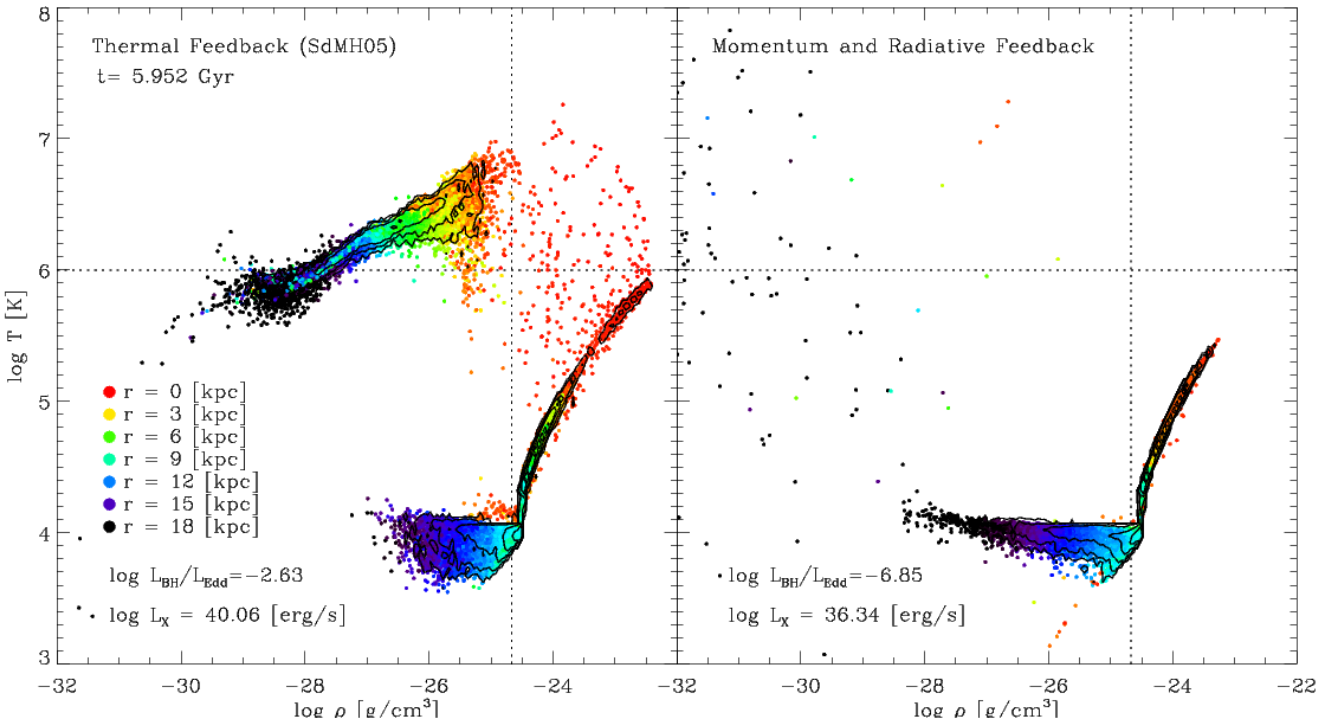

FIG. 5.— Distribution of gas in the density–temperature plane at $t = 5.95$ Gyr for the two feedback models. The radial distance from the BH is color coded, and the number density of SPH particles on the plot is shown with contours. The horizontal and vertical dotted lines respectively represent the temperature and density cuts we adopted for the X-ray luminosity estimate. Note that compared to the momentum feedback model, the thermal feedback model has much higher X-ray luminosity $L_{\rm X} \sim 3 \times 10^{40}$ erg s^{-1}, which is emitted from the diffuse hot gas, even during the low BH accretion phase ($L_{\rm BH}/L_{\rm Edd} \sim 0.002$).

long, and these hot and diffuse winds emit X-rays with the luminosity far greater ($\sim 10^{40}$ erg s^{-1}) than the momentum driven winds ($\sim 10^{36}$ erg s^{-1}). The momentum feedback model has much lower X-ray luminosity as the momentum-driven winds quickly expel the X-ray emitting hot gas. Even during the low BH accretion phase with $L_{\rm BH}/L_{\rm Edd} \sim 0.002$, the X-ray luminosity of the thermal feedback model is much higher than what is typically seen from normal massive spiral galaxies at the present epoch (10^{38}–10^{39} erg s^{-1} in the 0.5–2.0 keV band (Almy et al. 2000; Owen & Warwick 2009; Boroson et al. 2011)). The X-ray luminosity of the thermal feedback model is a lower bound, since the inclusion of cosmologically infalling gas in the simulations would lead to an increase in the computed thermal X-ray emission.

We now discuss the effect of the amount of the momentum-driven flow, i.e., number of momentum sharing neighbors in the momentum feedback model. As described in Section 2.2.2, we let the wind particle share its momentum with the neighboring gas particles, to mimic the shocked swept-up ambient medium. Because of the resolution limit, we keep the number of momentum sharing neighbors constant, despite the fact that a total swept-mass by momentum-driven wind depends on the mass of the BH (King 2003). In order to study the effect of the number of neighbors to share the momentum feedback, we ran a series of simulations adopting different numbers of neighbors. *We find that the effects of sharing momentum with more gas particles are small.* Adding more particles is equivalent to assuming an early and brief transition to the Sedov phase.

3.3. *Galaxy Merger Simulation*

In addition to isolated galaxies, we also performed an equal-mass galaxy merger simulation using our progenitor disk galaxy models. The merger simulation was ran at high numerical resolution (see Table 1) with the initial seed BH masses set at $10^5 M_\odot$. Following Johansson et al. (2009a) we adopt orbital geometry G13 (Naab & Burkert 2003) for our merger simulation. This geometry corresponds to the inclinations $i_p = -109, i_s = 180$ and the arguments of the pericenter $\omega_p = 60, \omega_s = 0$ for the primary and secondary galaxies, respectively. The galaxies approach each other on a parabolic orbit where the initial separation of the progenitors is $R_{\rm init} = r_{\rm vir}$ and the pericentric distance is $r_{\rm peri} = 2r_{\rm d}$, where $r_{\rm vir} = 160h^{-1}$ kpc is the virial radius and $r_{\rm d} = 2.5h^{-1}$ kpc is the disk scale radius. The simulation was evolved for a total of $t = 3$ Gyr with the merger taking place at $t \sim 1.5$ Gyr. The equal-mass merger initial conditions are simulated using both the standard thermal feedback and the new momentum mechanical feedback with the X-ray heating and radiation pressure.

In Figure 6, we show the evolution of the resulting total star formation (top), SMBH accretion (middle), and SMBH mass (bottom) for the two feedback models as a function of time. A similar evolution is seen in the star formation rate for both models, however the new feedback fiducial model has episodic outbursts of mass accretion as shown in the isolated galaxy model. Even though the two feedback models have different SMBH accretion history, the final mass of black hole is essentially the same. Other aspects of the two simulations, such as

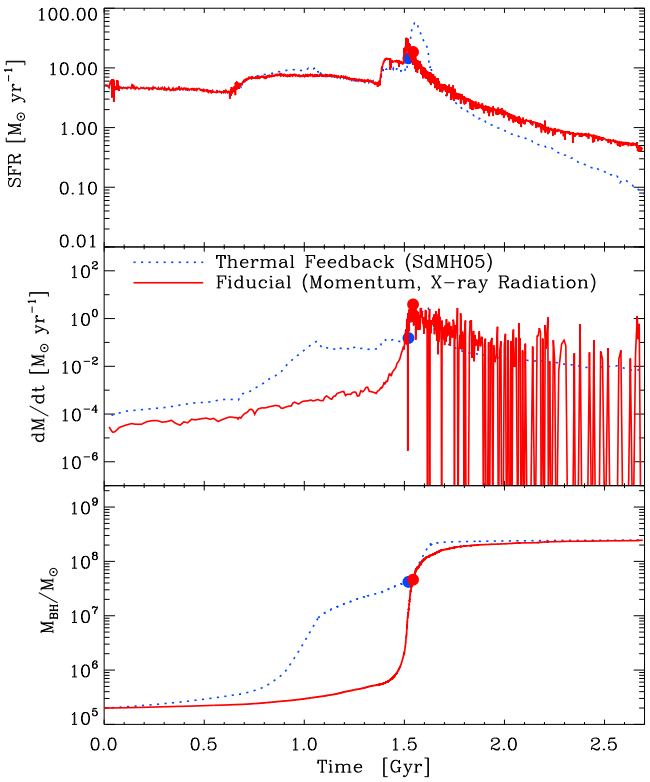

FIG. 6.— Comparison of the feedback models with a major merger of two galaxies: classical thermal feedback (blue), and our best proposed "Fiducial" model which has momentum mechanical feedback with the X-ray heating and radiation pressure (red). Evolution of the total star formation rate (top), the total accretion rate onto the black hole (middle) and the evolution of the black hole mass (bottom) are shown as a function of time for the 1:1 merger. The filled circles indicate the time of SMBH merger. Note that both the star formation rate and the black hole growth are essentially similar in the previous thermal feedback model and the new momentum driven treatment. However, the degree of fluctuation in the mass accretion rate is greater in the momentum feedback model as shown in the isolated galaxy case.

the X-ray thermal luminosity, are significantly different, and this will be discussed in later papers.

3.4. *Soft Bondi criterion*

Next, we turn our attention to the Bondi radius criterion. In order to test the new soft Bondi mechanisms for limiting accretion when numerical resolution is less than optimal, we ran two artificial test runs without any feedback, i.e., "No Feedback" models, with and without soft Bondi criterion. As discussed earlier in the Section 2.4.1, since any closest neighboring gas particles from the SMBH at any distance are considered as potentially accreting particles, gas particles keep accreting onto the SMBH and finally BH ends up swallowing all the gas in the host galaxy in the "No Feedback" model without soft Bondi criterion.

With the Bondi radius criterion added, we limit the accretion only to the gas particles statistically within the Bondi radius and we can prohibit the gas particles which are not within the gravitational influence of the BH from accreting onto the SMBH. In more realistic simulations which included feedback, the effects of our Bondi limitation are far less significant.

In Figure 7, we show the resulting SFRs, BH accretion rates, and BH mass growth for these two models with and

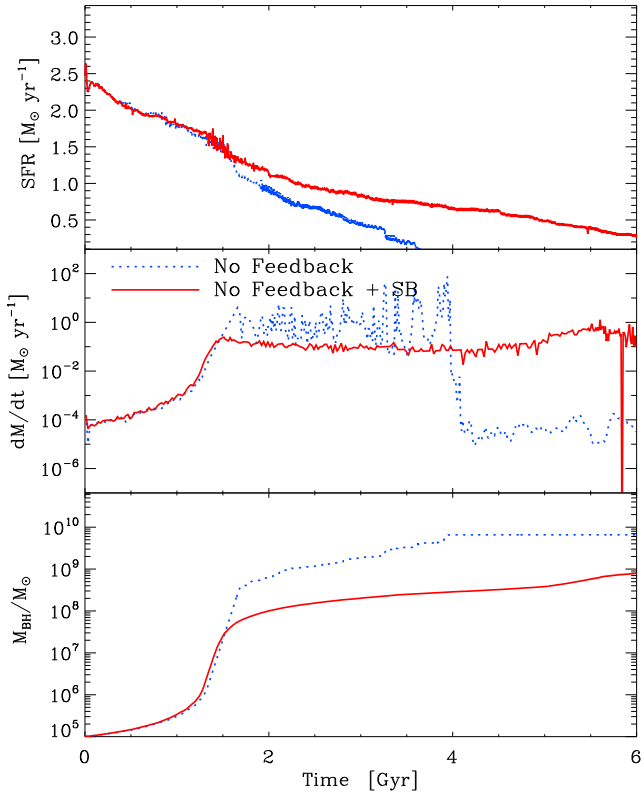

FIG. 7.— Comparison of the models with and without the Bondi radius criterion. Evolution of the global star formation rate (*top*), the accretion rate onto the black hole (*middle*) and the evolution of the black hole mass (*bottom*) are shown for each model. Note the order of magnitude reduction in the total accreted mass occasioned by including the Bondi limiter.

without the Bondi radius criterion. Utilizing the Bondi radius criterion effectively regulates the mass accretion, reducing the final mass by a factor of 10.

3.5. *Fiducial model and the effects of other physics*

In order to isolate and compare the effects of each feedback mechanism or modification made in the accretion, we perform the test simulations with one modification missing. In Figure 8, we show the temporal evolution of SFR, mass accretion rate onto BH and BH mass of three distinctive models, the one without radiative heating and radiation pressure (fiducial w/o XRP), the one without the Eddington force (fiducial w/o EF), and the one without the soft Bondi radius criterion (fiducial w/o SB), along with the fiducial model with all modifications as a reference. The radiative heating and radiation pressure is most effective among them, limiting the final mass of BH a factor of four. Compared to radiative feedback, both EF and Bondi criterion have minor effects on the final BH mass.

4. DISCUSSION

Absent a specific mechanism for transferring energy to particles surrounding an accreting BH, the AGN feedback via mass, and momentum output have not been included in classic thermal feedback works in three-dimensional hydrodynamic simulations. In this study, we have included the momentum mechanical feedback in the SPH simulation code, GADGET-2. We also include a treatment of the feedback by the X-ray radiation which

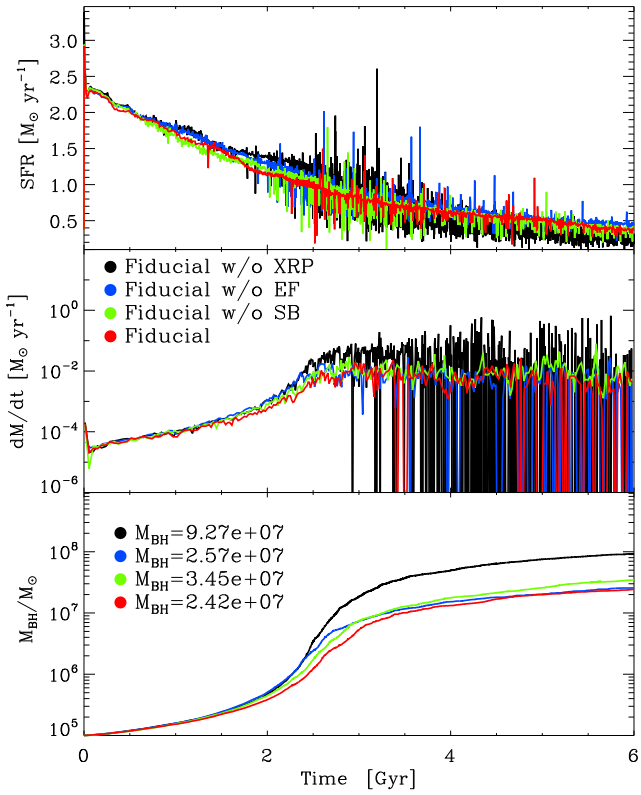

FIG. 8.— Various model comparison. Evolution of the global star formation rate (top), the accretion rate onto the black hole (middle) and the evolution of the black hole mass (bottom) in simulation of an isolated gas-rich galaxy. The largest of the newly included effects is clearly due to the X-ray heating and radiation pressure (XRP).

emanates from the BH and heats the surrounding gas in the host galaxies as well as radial momentum added to the fluid. We statistically limit accretion to gas particles which are gravitationally bound to the central BH (Bondi radius criterion).

A series of test simulations of isolated systems with new implementations of the momentum feedback and radiative feedback with new criteria on mass accretion are performed. Relevant quantitative properties of the models are presented in Table 2, while the general results can be summarized as follows.

1. Overall, the BH growth is quite similar in the two approaches, so the successful prediction of the $M_{\rm BH}-\sigma$ relation by Di Matteo et al. (2005, 2008) would be expected to be maintained in the new approach.

2. Our best proposed fiducial model with mechanical and radiative feedback by hard X-rays has much higher velocity outflows compared to the thermal feedback model, with $v_{\rm w}\sim 2000$ km s^{-1} and $L_{\rm wind}\sim 10^{42}$ erg s^{-1}. The total emitted kinetic energy of mechanical feedback model is ~ 100 times higher than that of the thermal feedback model, even when the same feedback energy coupling efficiency is assumed and the BH growth is similar. The outflows found in our fiducial model have properties broadly similar to those observed in some local Seyfert galaxies (Alatalo et al. 2011; Fischer et al. 2011; Müller-Sánchez et al. 2011).

3. The hot gas produced by slow, dense, thermally driven winds emits an X-ray luminosity significantly greater ($\sim 10^{40}$ erg s^{-1}) than the momentum-driven winds ($\sim 10^{36}$ erg s^{-1}). This X-ray luminosity of the thermal feedback model is also far greater than what is typically seen from normal spiral galaxies ($\sim 10^{38}$ erg s^{-1}; Almy et al. 2000; Owen & Warwick 2009).

4. In the mechanical feedback model, the fluctuation level in both radiant and wind outputs is considerably greater than in the standard thermal feedback model. While the thermal feedback model has a steady mass accretion with the Eddington ratio $L_{\rm BH}/L_{\rm Edd}=0.001$–$0.01$ throughout the simulations, the momentum feedback model has stochastic bursts in the mass accretion with the Eddington ratio, which spans from $L_{\rm BH}/L_{\rm Edd}=10^{-6}$ to 1.

5. In an artificial model computed without any feedback mechanisms (no feedback model), the SMBH grows to $\sim 10^{10}M_{\odot}$ accreting all the gas particles in the host galaxy. As noted, the standard prescription for accretion does not require the accreted particles be gravitationally bound to the central BH. However, the statistical implementation of the Bondi radius criterion can effectively limit the accretion of the gas particles to gravitationally bound particles, reducing the final mass of BH by a factor of 10. In more realistic models with feedback the differences are small.

6. Radiative heating and radiation pressure on the ISM by photons emitted by the central BH moderately reduces the final mass of BH, by a factor of four.

7. The growth of the BH is confirmed to be essentially the same in the thermal and momentum feedback models in an equal-mass galaxy merger simulations.

We benefited from useful conversations with D. Clay Hambrick, Taysun Kimm, Gregory S. Novak, Daniel Proga, and Silvia Pellegrini. We thank MPA Garching for generously extending hospitality to the first two authors for very productive scientific visits. An understanding of the standard approach was greatly aided by conversations with Lars Hernquist and we gratefully acknowledge Volker Springel and Lars Hernquist for the use of the SPH code. We thank the referee for many suggestions and comments which greatly improved this manuscript.

J.P.O. and E.C. acknowledge the support of NSF Grant AST-0707505. T.N. and E.C. acknowledge the support from the DFG cluster of excellence "Origin and Structure of the Universe". E.C. was supported by the Samsung Scholarship foundation and made extensive use of the computing facilities of the Princeton Institute of Computational Science and engineering. TN acknowledges support from the DFG priority program SPP1177. P.H.J. acknowledges the support of Research Funds of the University of Helsinki.

REFERENCES

Alatalo, K., Blitz, L., Young, L. M., et al. 2011, ApJ, 735, 88
Aller, M. C., & Richstone, D. O. 2007, ApJ, 665, 120
Almy, R. C., McCammon, D., Digel, S. W., Bronfman, L., & May, J. 2000, ApJ, 545, 290

Arav, N., Moe, M., Costantini, E., et al. 2008, ApJ, 681, 954
Barai, P., Proga, D., & Nagamine, K. 2011, MNRAS, 418, 591
Barway, S., & Kembhavi, A. 2007, ApJ, 662, L67
Bondi, H. 1952, MNRAS, 112, 195
Bondi, H., & Hoyle, F. 1944, MNRAS, 104, 273
Booth, C. M., & Schaye, J. 2009, MNRAS, 398, 53
Boroson, B., Kim, D.-W., & Fabbiano, G. 2011, ApJ, 729, 12
Chartas, G., Brandt, W. N., & Gallagher, S. C. 2003, ApJ, 595, 85
Ciotti, L., & Ostriker, J. P. 2007, ApJ, 665, 1038 (CO07)
Ciotti, L., Ostriker, J. P., & Proga, D. 2009, ApJ, 699, 89
Ciotti, L., Ostriker, J. P., & Proga, D. 2010, ApJ, 717, 708
Cox, T. J., Di Matteo, T., Hernquist, L., & Hopkins, P. F. 2006, ApJ, 643, 692
Crenshaw, D. M., Kraemer, S. B., & George, I. M., 2003, ARA&A, 41, 117
Dai, X., Shankar, F., & Sivakoff, G. R. 2008, ApJ, 672, 108
DeBuhr, J., Quataert, E., & Ma, C.-P. 2011, MNRAS, 412, 1341
DeBuhr, J., Quataert, E., & Ma, C.-P. 2012, MNRAS, 420, 2221
DeBuhr, J., Quataert, E., Ma, C.-P., & Hopkins, P., 2010, MNRAS, 406, L55
de Kool, M., Arav, N., Becker, R. H., et al. 2001, ApJ, 548, 609
Di Matteo T., Springel V., & Hernquist L. 2005, Nature, 433, 604
Di Matteo T., Colberg, J., Springel V., Hernquist L., & Sijacki, D. 2008, ApJ, 676, 33
Dressler, A. 1989, in IAU Symp. 134, Active Galactic Nuclei, ed. D. E. Osterbrock & J. S. Miller (Dordrecht: Kluwer), 217
Dubois, Y., Devriendt, J., Slyz, A., & Silk, J. 2009, MNRAS, 399, 49
Dubois, Y., Devriendt, J., Slyz, A., & Teyssier, R. 2012, MNRAS, 420, 2662
Dunn, J. P., Bautista, M., Arav, N., et al. 2010, ApJ, 709, 611
Durier, F., & Dalla Vecchia, C. 2012, MNRAS, 419, 465
Fabian, A. C. 1999, MNRAS, 308, 39
Fischer, T. C., Crenshaw, D. M., Kraemer, S. B., et al. 2011, ApJ, 727, 71
Gebhardt, K., Bender, R., Bower, G., et al. 2000, ApJ, 539, L13
Gibson, R. R., Jiang, L., Brandt, W. N., et al. 2009, ApJ, 692, 758
Graham, A. W., Onken, C. A., Athanassoula, E., & Combes, F. 2011, MNRAS, 412, 2211
Greene, J. E., & Ho, L. C. 2007, ApJ, 667, 131
Gültekin, K., Richstone, D. O., Gebhardt, K., et al. 2009, ApJ, 698, 198
Haardt, F., & Madau, P. 1996, ApJ, 461, 20
Hambrick, D. C., Ostriker, J. P., Naab, T., & Johansson, P. H. 2011, ApJ, 738, 16
Hernquist, L. 1990, ApJ, 356, 359
Hewitt, P. C., & Foltz, C. B. 2003, AJ, 125, 1784
Ho, L. C. 2009, ApJ, 699, 626
Holt, J., Tadhunter, C. N., & Morganti, R. 2008, MNRAS, 387, 639
Hopkins, P. F., Hernquist, L., Cox, T. J., et al. 2005, ApJ, 630, 705
Hoyle, F., & Lyttleton, R. A. 1939, Proc. Camb. Phil. Soc., 34, 405
Janiuk, A., Sznajder, M., Mościbrodzka, M., & Proga, D. 2009, ApJ, 705,1503
Johansson, P. H., Burkert, A., & Naab, T. 2009a, ApJL, 707, 184
Johansson, P. H., Naab, T., & Burkert, A. 2009b, ApJ, 690, 802
Katz, N., Weinberg, D. H., & Hernquist, L. 1996, ApJS, 105, 19
Kauffmann, G., & Heckman, T. M. 2009, MNRAS, 397, 135
Kim, J.-H., Wise, J. H., Alvarez, M. A., & Abel, T. 2011, ApJ, 738, 54
King, A. 2003, ApJ, 596, L27
Kormendy, J. 1993, in The Nearest Active Galaxies, ed. J. Beckman, L. Colina., & H. Netzer (Madrid: Consejo Superior de Investicaciones Cientificas), 197
Kormendy, J., & Richstone, D. 1995, ARA&A, 33, 581
Krolik, J. H., & Begelman, M. C. 1988, ApJ, 329, 702
Lynden-Bell, D. 1969, Nature, 223, 690
Magorrian, J., Tremaine, S., Richstone, D., et al. 1998, AJ, 115, 2285
Marconi, A., & Hunt, L. K. 2003, ApJ, 589, L21
Mckee, C. F. & Ostriker, J. P. 1977, ApJ, 218, 148
Moe, M., Arav, N., Bautista, M. A., & Korista, K. T. 2009, ApJ, 706, 525
Monaghan, J. J. 1992, ARA&A, 30, 543
Müller-Sánchez, F. Prieto, M. A., Hicks, E. K. S., et al. 2011, ApJ, 739, 69
Naab, T. & Burkert, A. 2003, ApJ, 597, 893
Navarro, J. F., Frenk, C. S., & White, S. D. M. 1995, MNRAS, 275, 720
Navarro, J. F., Frenk, C. S., & White, S. D. M. 1997, ApJ, 490, 493
Nayakshin, S., & Power, C. 2010, MNRAS, 402, 789
Nobel, S. C., Krolik, J. H., & Hawley, J. F. 2009, ApJ, 692, 411
Novak, G. S., Ostriker, J. P., & Ciotti, L., 2011, ApJ, 737, 26
Omma, H., Binney, J., Bryan, G., & Slyz, A. 2004, MNRAS, 348, 1105
Ostriker, J. P., Choi, E., Ciotti, L., Novak, G. S., & Proga, D. 2010, ApJ, 722, 642 (OCCNP10)
Owen, R. A., & Warwick, R. S. 2009, MNRAS, 394, 1741
Pounds, K. A., Reeves,, J. N., King, A. R., et al. 2003, MNRAS, 345, 705
Pounds, K. A., & Vaughan, S. 2011, MNRAS, 413, 1251
Proga, D., & Kallman, T. R. 2004, ApJ, 616, 688
Proga, D., Ostriker, J. P., & Kurosawa, R. 2008, ApJ, 676, 101
Proga, D., Stone, J. M., & Kallman, T. R. 2000, ApJ, 543, 686
Rees, M. J. 1984, ARA&A, 22, 471
Richstone, D., Ajhar, E. A., Bender, R., et al. 1998, Nature, 395, 14
Saitoh, T. R., & Makino, J. 2009, ApJ, 697, L99
Sazonov, S. Y., Ostriker, J. P., & Sunyaev, R. A. 2004, MNRAS, 347, 144
Sazonov, S., Y., Ostriker, J. P., Ciotti, L., & Sunyaev, R. A. 2005, MNRAS, 358, 168
Shakura, N. I., & Sunyaev, R. A. 1973, A&A, 24, 337
Sijacki, D., Springel, V., Di Matteo, T., & Hernquist, L. 2007, MNRAS, 380, 877
Soltan, A. 1982, MNRAS, 200, 115
Springel, V. 2005, MNRAS, 364, 1105
Springel, V. 2010, ARA&A, 48, 391
Springel, V., Di Matteo, T., & Hernquist, L. 2005a, ApJ, 620, L79
Springel, V., Di Matteo, T., & Hernquist, L. 2005b, MNRAS, 361, 776 (SdMH05)
Springel, V., & Hernquist, L. 2003, MNRAS, 339, 289
Tacconi, L. J., Genzel, R., Blietz, M., et al. 1994, ApJ, 426, L77
Teyssier, R., Moore, B., Martizzi, D., Dubois, Y., & Mayer, L. 2011, MNRAS, 414, 195
Tremaine, S., Gebhardt, K., Bender, R., et al., 2002, ApJ, 574, 740
Younger, J. D., Hopkins, P. F., Cox, T. J., & Hernquist, L. 2008, ApJ, 686, 815
Yu, Q., & Tremaine, S. 2002, MNRAS, 335, 965

APPENDIX

ACCRETION MODEL

We test our modified model of unresolved accretion onto the BH summarized in Section 2.4. Our simulation set-up consists of a random distribution of gas particles in a periodic box with an accreting BH particle in the center. The size of the box is 1 kpc, and 20000 gas particles with a mass of 2750 $M_\odot$ are used for the simulations. The mass of each gas particles is ~ 30 times smaller than that of our galaxy simulation model at standard resolution, and the gravitational softening length is ~ 5 pc. We choose $M_{\rm BH} = 4 \times 10^6 M_\odot$ and the corresponding initial Bondi radius (Equation (21)) is $r_{\rm Bondi} = 10$ pc, with $T_{\rm gas}$=20000 K and Gaussian velocity distribution with $\bar{v}_{\rm gas} = 50$ km/s and $\sigma_{v,{\rm gas}} = 5$ km/s. No radiative cooling is considered and dimensionless accretion parameter α is set to be 1.

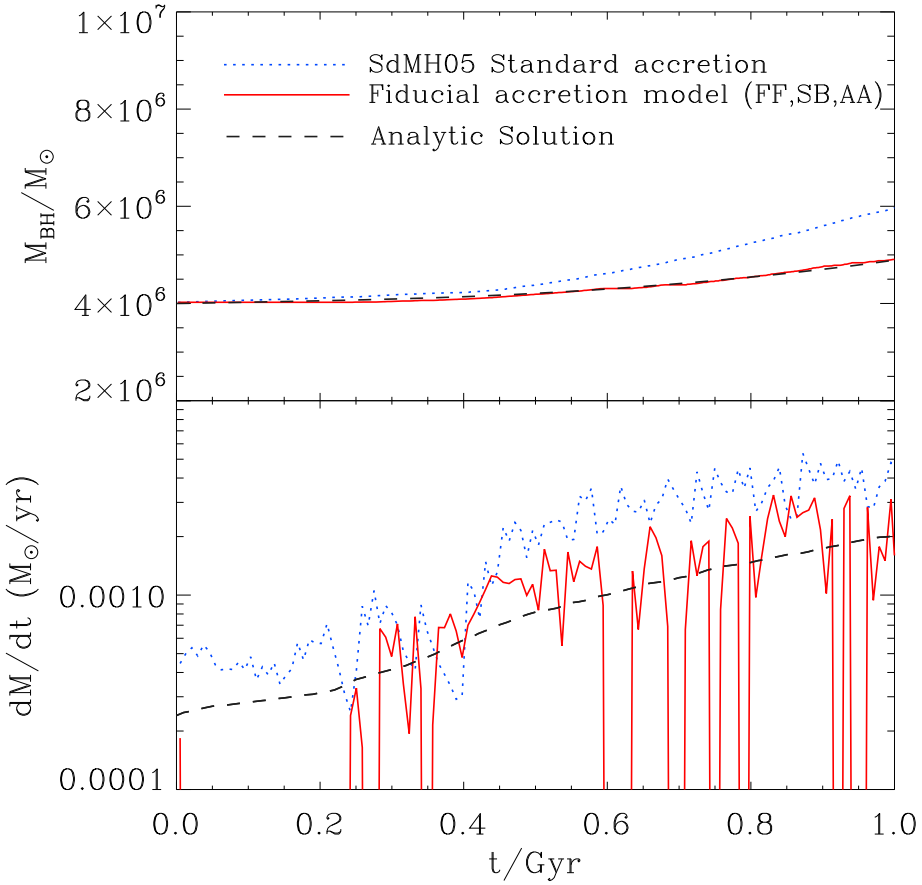

FIG. 9.— Evolution of the black hole masses (top) and mass accretion rates onto BH (bottom) of the simulations of mass accretion models. The standard mass accretion model described in Section 2.2 in this paper (refer to SdMH05 for details), and new accretion model with all of modifications we described for the BH mass accretion model, i.e., soft Bondi radius criterion (SB), free-fall modification (FF), and alternative averaging (AA) (see Section 2.4). The integrated new accretion model (red) agrees well with the analytic expectation despite the fact that the instantaneous accretion rate is often higher due to the intervals when the instantaneous rate is zero.

We perform a direct comparison of our new accretion model with the SdMH05 model. In Figure 9, we plot the resulting BH accretion rate, and total BH mass for the simulation performed using the standard mass accretion model described in SdMH05, and compare it to the corresponding output of the accretion model presented in this paper (with FF, SB radius criterion, and AA following Equations (24) and (25)). We also plot the analytic solution of the mass accretion of a given physical properties, i.e., Bondi solution which is described in the analytical formula of Bondi (1952) under the assumption of spherical symmetry and negligible angular momentum as,

$$\dot{M}_{\rm B} = \lambda 4\pi r_{\rm Bondi}^2 \rho_\infty c_{s,\infty}, \tag{A1}$$

where the dimensionless parameter λ depends only on the adiabatic index of the accreting gas (for details, see Bondi (1952); Janiuk et al. (2009)). For an assumed adiabatic index $\gamma = 5/3$, $\lambda = 0.25$ (Bondi 1952).

The evolution of the BH mass as a function of time for the new accretion model agrees well with that of the analytic Bondi solution. The total accreted gas mass for the previously used accretion model is about two times larger. As shown in the bottom panels of Figure 9, in the standard mode the mass is accreted continuously whereas in our fiducial model we have discrete accretion events. That is mainly because the soft Bondi radius criterion prohibits the gas particles which are not within the gravitational influence of the BH from accreting onto the BH and stops the accretion before the gas particles are found statistically within the Bondi radius. The new model does not have mass accretion for the first ~ 0.2 Gyr, before the accretion flow is formed around the BH in the center. Even if the Bondi radius is not fully resolved as in many of the applications, we obtain the Bondi solution with our new BH statistical mass accretion prescription. Given the discrete nature of our particles the accretion rate is inevitably stochastic. However, the computed accretion rate closely follows the exact analytic solution when we adopt our statistical treatment.